NASA Contractor Report 3000

Preliminary Investigation of Crack Arrest in Composite Laminates Containing Buffer Strips

James G. Goree

GRANT NSG-1297
MAY 1978

NASA

TABLE OF CONTENTS

LIST OF FIGURES

LIST OF FIGURES (Cont'd)

LIST OF TABLES

SUMMARY

The experimental determination of the mechanical properties of some specific composite laminates and a preliminary investigation of the crack arrest potential of laminates containing buffer strips are considered.

All laminates used in the material property portion of the investigation were eight ply, constructed from single-ply tape containing unidirectional fibers preimpregnated in 177°C cure Rigidite 5208 epoxy resin.[1] The basic, or parent, laminate was graphite/epoxy, and the hybrid materials were S-glass, E-glass and Kevlar-49.[2] Standard test coupons 5.08 cm wide by approximately 25.4 cm long were used. The tests were performed under static loading and room temperature, dry conditions. Tabulated values for elastic properties and stress intensity values are given, as well as complete stress/strain curves for each laminate tested. The experimentally determined values of the elastic properties are compared with the values calculated using classical lamination theory and good agreement is shown for those laminates exhibiting linear stress/strain behavior. Some comments are made concerning the connection between ply delamination and fracture toughness, both as observed in the present study, and as noted by other investigators.

---

[1]Rigidite 5208: Registered trademark of Narmco Materials Inc.

[2]Kevlar-49: Registered trademark of E. I. du Pont de Nemours & Co., Inc.

The buffer strip laminates for the crack arrest portion of the study were fabricated using six layers of woven fiber glass cloth and room temperature cure polyester resin. Each laminate was approximately 30.5 cm by 30.5 cm and contained two buffer strips formed by interrupting the cloth and weakening the inner laminar bond with Teflon-coated glass fabric.[3] Woven Kevlar cloth was also used in place of the fiberglass buffer strips. Results indicating that a weak interface bond does enhance crack arrest were observed.

---

[3]Teflon: Registered trademark of E. D. du Pont de Nemours & Co., Inc.

I. INTRODUCTION

In investigations concerning the potential use of composite materials in advanced structures, considerable attention has been given to problems associated with damage or flaws and the resulting fatigue and fracture characteristics of the composite. The need for the capability to design damage tolerant composite structures with at least the same degree of confidence as now exists for metallic structures is essential if such materials are to be used in production.

For composite laminates, the technique of hybrid material buffer strips embedded at regular intervals throughout the laminate has been demonstrated, for example see [1], to have the capability of arresting through-the-laminate cracks, and in some cases gives a residual strength approaching the net section capacity of the laminate. The mechanism associated with the crack arrest and ultimate failure of such laminates has not, however, been explained nor have satisfactory methods been developed to allow for accurate prediction of crack arrest loads or ultimate failure in terms of the laminate geometry and materials.

This is in contrast with the analogous design for metallic structures in which case either bonded or riveted stringers are added to the metal panel without significantly interrupting the continuity of the basic panel. The panel and stringers then act much more independently during crack

growth and fracture than appears to be the case in composite laminates with internal buffer strips. A detailed investigation of the problem of riveted stringers reinforcing a cracked isotropic elastic sheet is presented in [2]. A similar study concerning composite laminates with buffer strips has not, to the knowledge of this writer, been completed.

The purpose of the present study was to investigate experimentally the mechanical properties of specific composite laminates as part of an overall program to study, both analytically and experimentally, the nature of crack arrest and failure in composite panels with buffer strips. Due to its widespread use in advanced composite structures, T-300 graphite with an epoxy matrix was chosen as the parent laminate material. Three additional fibers, 1014 S-glass, E-glass, and "Kevlar-49" were chosen as being representative of suitable buffer strip materials. All laminates in this part of the study were eight-ply using NARMCO 5208 (177 C° cure) epoxy resin.

In order to gain some further insight into the mechanisms associated with crack arrest at an internal hybrid buffer strip in a laminate, a limited series of tests were also developed using fiberglass/polyester laminates containing two buffer strips each. The panels were designed in an attempt to study the effects of the strength of the interface bond between laminae in the buffer strips on crack arrest,

as it appears that the coupling of adjacent laminae due to the presence of interface normal and shear stresses significantly increases the potential for crack growth. It was then planned to weaken this interface coupling by adding strips of Teflon-coated glass cloth between laminae in the buffer strip regions. Hybrid buffer strips of Kevlar woven cloth replacing the glass fabric were also used, both with and without the Teflon-coated glass cloth.

Considerable analytical work has been done for both isotropic and orthotropic materials in investigating the stresses in the vicinity of a crack tip for the crack being near, at, crossing or along a material interface. (See [3], [4], [5], [6], and [7].) These studies considered the laminate as a thin homogeneous isotropic or orthotropic plane and investigated the resulting two-dimensional stress state. Through the thickness variations in material properties and stresses were not considered. It appears that for the imbedded hybrid buffer strip the significant stresses are, in fact, the interlaminar stresses and the three-dimensional problem must be considered. It does not seem reasonable to expect to develop a general solution in the manner of the above mentioned two-dimensional studies, as the extension to a three-dimensional stress state with finite thickness would be exceedingly complicated.

Some possibility of success might be had in modeling the laminate as in classical lamination theory, where, as

discussed in [8], [9], and [10], the interlaminar stresses near a free edge of a laminate have been approximated. Finite element or finite difference solutions also are a possibility; however, without some improvements in the current three-dimensional programs to account for through-the-thickness variations, the computation time seems prohibited. A different approach which appears to have some potential is to model the laminae as in [11], [12], and [13], resulting in differential-difference equations with the most significant characteristics of the fibers and the matrix accounted for. An attempt to model a three-dimensional laminate in this fashion will be attempted in the continuation of this investigation.

A significant part of the justification for the current experimental study was to develop a better understanding of the behavior of laminates in order to be able to model more accurately the three-dimensional stress problem.

Certain commercial materials are identified in this paper in order to specify adequately which materials were investigated in the research effort. In no case does such identification imply recommendation or endorsement of the product by NASA, nor does it imply that the materials are necessarily the only ones or the best ones available for the purpose.

The writer wishes to express his appreciation to the National Aeronautics and Space Administration for the support of this investigation under NASA Grant NSG-1297.

The generous use of the autoclave facilities provided by the Lockheed-Georgia Company is also acknowledged.

II. HYBRID/GRAPHITE/EPOXY LAMINATES

A. Construction of Laminates

Relatively large panels of each material and geometric configuration were fabricated such that two duplicate coupons could be obtained for almost all particular material property tests. The laminate designation, test coupon size and material/geometric construction is given in Table 1. The particular test coupon designation is shown in Figures 1 and 2.

The first test laminates were from unidirectional panels of each of the four chosen materials and were designated A1 for graphite, A2 for S-glass, A3 for E-glass, and A4 for Kevlar. The second set of coupons were from all $\pm 45°$ panels of each of the four materials and were designated B1, B2, B3 and B4 for all graphite, S-glass, E-glass, and Kevlar, respectively. There were four panels each in groups A and B and four test coupons cut from each panel giving thirty-two coupons as indicated in Figure 1. All coupons in groups A and B were loaded in the zero degree direction.

The "hybrid laminates" consisted of eight panels, each of which contained eight test coupons as shown in Figure 2 and defined in Table 1. The first four panels were of quasi-isotropic construction $[90°, \pm 45°, 0°]_s$ with panel C1 being all graphite and panels C2, C3 and C4 being hybrid laminates formed by replacing the two center 0° laminae with S-glass,

E-glass and Kevlar, respectively. The last four panels were fabricated as [90°, $\pm$45°, -45°, +45°, $\mp$45°, 90°] and were the only unsymmetrical laminates. Panel D1 was all graphite and panels D2, D3, and D4 were again hybrid laminates formed by replacing the center -45°, +45° laminae with S-glass, E-glass and Kevlar respectively. Laminates from panel C1 are referred to as "parent" laminates with a major emphasis of the test being to determine the change in elastic properties between test coupons from the seven "hybrid" laminates C2, C3, C4, D1, D2, D3 and D4 and the corresponding coupon from the "parent" laminate C1. There were eight of the above panels, each containing eight test specimens or sixty-four coupons from the hybrid panels. The direction of loading for the coupons in groups C and D was either zero or ninety degrees as indicated in Figure 2 and designated as Cn-0, Dn-0 for zero degree loading and Cn-90, Dn-90, for ninety degree loading.

All panels were fabricated using 7.62 cm wide unidirectional preimpregnated tape (slit net), which had an accuracy of $\pm$ 0.076 cm across the width. Cured ply thickness was estimated by the vendor to be 0.013 cm for all but E-glass which was 0.023 cm. Cured laminate dimensions agreed closely with this as seen in Table 1.

Sections of the uncured preimpregnated tape were analyzed by the chemistry department of Clemson University to ascertain the fiber to resin ratio by weight. These results

agreed quite closely with the ratios reported by the vendor as seen in Table 2.

Laminates of group A were fabricated as 21.6 cm wide by 26.7 cm long panels, those of group B were 21.6 cm wide by 21.6 cm long, and group C and D panels were 26.7 cm wide by 41.91 cm long. The lay-up for all laminates was begun by placing a nylon peel ply on the work surface. A carpenter's square was used to provide a common edge for the eight laminae and fiber orientation was established with the use of a drafting triangle.

Three and a half strips of tape were used per ply in laying up the unidirectional laminates in groups A. The stacking arrangement shown in Figure 3 provided an overlapping strip at each place where two edges of the tape came together.

Panels of all plus-minus forty-five degrees, group B, were constructed of alternating plies made of four strips of tape as shown in Figure 4. The center two plies were both minus forty-five degrees to provide mid-plane symmetry.

Groups C and D panels were begun with a ninety degree lamina using five and a half strips of the tape, and the forty five degree plies were constructed of seven strips as shown in Figure 5. The center plies of the group C laminates, when orientated at zero degrees, were stacked as in the unidirectional laminates. When the center plies were at forty-five degree, they were constructed similar to the second and third layers, and were the only panels not having mid-plane symmetry.

When the lay-up was completed, each panel was covered with a nylon peel ply and prepared for curing. Platens were made from aluminum. Each platen was mechanically sanded and hand polished to obtain a mirror finish and coated with a mold release. The laminate was placed on it's platen and surrounded by a cork edge dam to control resin flow during the curing cycle. A layer of Teflon-coated glass cloth, fiber-glass bleeder cloth (style 181), and a pressure plate made from 0.160 cm aluminum were then fitted inside the edge dam. A release film was draped over the plate and secured to the edge dam using masking tape. This arrangement is shown in Figure 6, and the curing cycle is shown in Table 3. The fiberglass breather cloth and vacuum bag were provided by Lockheed of Marietta, Georgia, along with the use of their autoclave facilities. This curing method produced approximately fifty per cent unuseable material. Excess resin accumulated on the platens such that several of the laminate panels could not be removed. Further damage resulted from the outer layer, platen side, of the laminates adhering to the peel ply when it was removed. Because of this damage, there were no D2-90 coupons. Replacements for the remaining damaged panels were laid-up as described earlier, but the curing method was modified as shown in Figure 7. Using bleeder cloth and Teflon-coated glass on both sides of the laminate panel resulted in one hundred per cent useable material and provided a better surface for

mounting strain gages and attaching end tabs. The autoclave cycle used for the modified curing method is shown in Table 4. Final thickness of the laminates was essentially the same for the two methods, and material properties were within the range of the experimental scatter.

The chemistry department attempted to measure the fiber to resin ratio by weight of the finished laminates, but were unsuccessful with attempts to dissolve cured samples. Based on discussions with the vendor, the cured laminates were estimated to be approximately seventy-four per cent fiber by weight, or sixty per cent fiber by volume.

A post cure was suggested by the vendor; however, this is shown in [1] to offer no improvement in mechanical properties when the laminates were used (tested) at room temperature. It was then decided that the post cure could be omitted without introducing any measureable effects. For elevated temperature and with absorbed moisture in the matrix, the post cure is significant.

B. Test Specimen Preparation

The panels were cut into 5.08 cm wide coupons using a surface grinder initially fitted with a 0.160 cm thick by 15.25 cm diameter diamond cutting wheel. This wheel had a diamond section depth of 0.32 cm with a one hundred grit size and was operated at 3000 rpm. Attempts to cut the panels in groups A and B resulted in the diamond wheel becoming saturated from both the glass and "Kevlar". No difficulty was experienced with the graphite. This caused overheating and cracking of the wheel around the rim. A standard, seventy grit, cutting wheel, which is self cleaning in that the diameter is constantly reduced by wear, was found to be satisfactory for all the remaining laminates. Panels in groups A and B produced four coupons each as shown in Figure 1 and groups C and D panels produced eight coupons each as shown in Figure 2. Due to a cutting error by shop personnel, there were no D4-0 coupons.

The end tabs were constructed using 5.08 cm squares of 0.160 cm aluminum bonded to the coupons with 121°C cure adhesive film. After bonding, the tabs were milled to a uniform thickness to prevent bending from misalignment in the testing machine. Only one failure was experienced with the aluminum tabs during the tests. As an initial trial, end tabs of 0.635 cm plexiglas were bonded to a coupon using urethane air cure glue, however, the glue failed at

approximately 8 000N, which was well below the load carrying capacity of most of the coupons.

Coupons three, six and seven of the groups C and D panels and one coupon from each A and B panel were used to determine the stress intensity factors. These coupons were notched using a 0.238 cm end mill to give a 1.27 cm center notch through the coupon as shown in Figure 8.

Two coupons of the same construction, from which stress/strain values were obtained, were prepared by mounting both longitudinal and transverse strain gages on each side as shown in Figure 9. The gages had a resistance of 350 ohms, a gage length of 3.18 mm, and a self-temperature-compensation of $1.08 \times 10^{-5}\ K^{-1}$.

C. Testing Procedure

The specimens were loaded in a 434 000 N universal testing machine. Stress/strain relationships were obtained by slowly incrementing the load such that it was essentially static. At each increment, readings from the four strain gages were manually recorded. Tests to determine the stress intensity factors were conducted by loading each coupon until complete failure.

D. Test Results

The experimentally determined stress/strain diagrams are given in Figures 10, 11, 12 and 13. Figure 10 corresponds to the unidirectional laminates, group A, with the load being in the fiber (zero degree) direction. Figure 11 gives the stress/strain relationship for the $\pm 45°$, group B, laminates also under the action of a uniaxial (zero degree) load. The hybrid laminates of groups C and D are presented together in Figures 12 and 13 where Figure 12 gives the results for zero degree loading and Figure 13 for transverse (ninety degree) loading.

Moduli of Elasticity and Possion's ratios both as measured from the above stress/strain diagrams and as computed from classical lamination theory [8] are given in Tables 5 and 6. Stress intensity factors for the notched laminates are presented in Table 7. A brief discussion of classical lamination theory is given in section E of this report.

All elastic properties were computed using the 0.2 percent strain offset method and the Poisson's ratios were determined at the 0.2 percent strain level.

The stress/strain curves were found to be essentially linear over the full range of loading, except for the group B ($\pm 45°$) laminates. The calculated values of material properties agree quite well with the measured values for

the linear materials as can be seen from Tables 5 and 6. It should be noted that in calculating the elastic properties using classical lamination theory, the lamina properties E_{11} and ν_{12} as measured for the group A laminates were used for the known unidirectional lamina properties. The unidirectional lamina shear modulus G_{12} and transverse modulus E_{22} was not measured and average values obtained from the vendor were used. The transverse Poisson's ratio for a lamina was then computed as $\nu_{21} = \nu_{12}E_{22}/E_{11}$.

Examination of the stress/strain curves seem to indicate that failure of the un-notched coupons occurs at a strain level close to that of the lowest strain-to-failure lamina in the laminate. It is interesting to note that the zero degree graphite (A1) and $\pm 45°$ graphite (B1) both fail at approximately 0.95 per cent strain which is also the strain-to-failure of the 5208 resin alone (1.0% as obtained from the vendor). It appears then that for the $\pm 45°$ graphite fibers, the bending and distortion introduced by the matrix failure results in fiber failure at an axial fiber strain considerably less than the corresponding uniaxial strain-to-failure as determined from the group A laminates. For this same laminate at elevated temperature and high moisture content, the strain-to-failure of the matrix increases drastically; i.e., for temperatures above the glass transition point for the epoxy matrix, strain-to-failure on the order of 10-15% has been observed. Under these conditions, the behavior of the $\pm 45°$ specimen could be expected to change

considerably with much larger strain of the laminate and with significant reduction in cross-section of the coupon. For the present room temperature, dry test, very little reduction in cross-section was observed for any of the coupons. In fact, for the four materials tested, the E-glass (A3, B3) was the only one in which strain-to-failure for the $\pm 45°$ laminates was greater than the corresponding value for the 0° laminates.

For the hybrid laminates, groups C and D, the coupling between laminae reduces the strain-to-failure of the laminate in the direction of loading in all cases. In the instance of a transverse load, as depicted in Figure 13, all coupons failed at nearly the same strain of about 0.8 percent which is less than the 0.95 per cent for unidirectional graphite.

It should be noted that the scale on the stress-strain diagrams is different on each curve due to the considerable change in load range.

A more significant part of these tests was perhaps the investigation of notch sensitivity of the various laminates and the observations indicating their suitability as potential candidates for buffer strip material. Stress intensity factors, K_1, were computed for the coupons as described by Newman in [14], to account for the finite width of the coupon.

$$K_1 = \sigma\sqrt{\pi a}\ F$$

where $\sigma = P/wt$, a = crack half-length, P = axial load, W = coupon width, t = coupon thickness and F = finite width correction factor from Table VII of [14].

For all laminates tested, a = 0.635 cm, w = 5.08 cm, t = thickness of the particular coupon, and F = 1.0416.

These factors are presented in Table 7 along with the ultimate stress of the coupons, and the net section average stress-at-failure.

All four unidirectional laminates of group A were observed to be insensitive to a center notch and in none of the tests did a self-similar crack originate at the notch. The ultimate and net section average stress of the notched unidirectional graphite and S-glass were not obtained as both coupons failed near the grips at a reduced stress.

Laminates in group B all failed along forty-five degree lines passing through the notch ends, with some delamination occurring between the plies. Net section average stress-at-failure agreed closely with the un-notched ultimate stress for the glass and "Kevlar" as the effect of the notch was mainly a reduction in cross section area. The all forty-five degree graphite was most affected by the center notch

as the net section average stress-at-failure was twenty-six per cent less than the ultimate stress of the un-notched specimen.

Notch sensitivity of the C and D group coupons was demonstrated by comparing the net section stress-at-failure with that of the parent laminate (C1). As shown in Table 7, for the Cn-0 coupons, with the center plies parallel to the load, S-glass and "Kevlar" had the least reduction in net section stress-at-failure . From this it seems that they would perhaps be the best buffer strip materials. However, it was observed that S-glass and E-glass delaminated more than "Kevlar", and the delamination of the glass plies in C2-0 and C3-0 had the same appearance as buffer strips which were shown to arrest cracks in 1 . The Dn-0 coupons, with forty-five degree center plies, did not produce significant delamination, and the net section average stress-at-failure was significantly less than that of C1-0. The Cn-90 and Dn-90 coupons were all notch sensitive, and failure resulted in self-similar cracks growing outward from the center notch. Again, very little delamination was observed.

E. CLASSICAL LAMINATION THEORY

A complete description of the development of the macromechanical behavior of a laminate is covered in [8] where the resultant normal forces and twisting moments are shown to be related to the laminate middle surface strains and rotations by the following equations.

$$\begin{Bmatrix} N_x \\ N_y \\ N_{xy} \end{Bmatrix} = \begin{bmatrix} A_{11} & A_{12} & A_{16} \\ A_{12} & A_{22} & A_{26} \\ A_{16} & A_{26} & A_{66} \end{bmatrix} \begin{Bmatrix} \varepsilon_x^o \\ \varepsilon_y^o \\ \gamma_{xy}^o \end{Bmatrix} + \begin{bmatrix} B_{11} & B_{12} & B_{16} \\ B_{12} & B_{22} & B_{26} \\ B_{16} & B_{26} & B_{66} \end{bmatrix} \begin{Bmatrix} \kappa_x \\ \kappa_y \\ \kappa_{xy} \end{Bmatrix}$$

$$\begin{Bmatrix} M_x \\ M_y \\ M_{xy} \end{Bmatrix} = \begin{bmatrix} B_{11} & B_{12} & B_{16} \\ B_{12} & B_{22} & B_{26} \\ B_{16} & B_{26} & B_{66} \end{bmatrix} \begin{Bmatrix} \varepsilon_x^o \\ \varepsilon_y^o \\ \gamma_{xy}^o \end{Bmatrix} + \begin{bmatrix} D_{11} & D_{12} & D_{16} \\ D_{12} & D_{22} & D_{26} \\ D_{16} & D_{26} & D_{66} \end{bmatrix} \begin{Bmatrix} \kappa_x \\ \kappa_y \\ \kappa_{xy} \end{Bmatrix} \quad (1)$$

The A_{ij} are the extensional stiffnesses, the B_{ij} are the coupling stiffnesses and the D_{ij} are the bending stiffnesses. The coupling stiffnesses, B_{ij} corresponds to a coupling between the bending and twisting of a laminate. For a laminate whose individual laminae are symmetrically placed with respect to the midplane, no coupling will exist and the B_{ij} will be zero. The group D laminates of the present study are the only ones which are not symmetric and the

degree of non-symmetry is very small due to the six symmetric laminae. Very little out of plane deformation was noted on any of the test coupons during loading.

In the above equations, the resultant forces N_x, N_y, N_{xy} are related to the average, through the laminate, stresses as

$$\begin{Bmatrix} N_x \\ N_y \\ N_{xy} \end{Bmatrix} = \int_{-t/2}^{t/2} \begin{Bmatrix} \sigma_x \\ \sigma_y \\ \sigma_{xy} \end{Bmatrix} dZ = t \begin{Bmatrix} \sigma_x^{\,o} \\ \sigma_y^{\,o} \\ \sigma_{xy}^{\,o} \end{Bmatrix} \tag{2}$$

where σ_x, σ_y, σ_{xy} are actual stresses and $\sigma_x^{\,o}$, $\sigma_y^{\,o}$, $\sigma_{xy}^{\,o}$ are average stresses. The laminate thickness is denoted by t.

For a symmetrical laminate ($B_{ij} = 0$), and the average strains are related to the average stresses by inverting equation (1) as

$$\begin{Bmatrix} \varepsilon_x^{\,o} \\ \varepsilon_y^{\,o} \\ \gamma_{xy}^{\,o} \end{Bmatrix} = \begin{bmatrix} A_{11}^{-1} & A_{12}^{-1} & A_{16}^{-1} \\ A_{12}^{-1} & A_{22}^{-1} & A_{26}^{-1} \\ A_{16}^{-1} & A_{26}^{-1} & A_{66}^{-1} \end{bmatrix} \begin{Bmatrix} N_x \\ N_y \\ N_{xy} \end{Bmatrix} \tag{3}$$

where A_{ij}^{-1} = cofactor of $A_{ij}/|A|$, $|A|$ is the determinant of [A].

Then, if the laminate is fabricated such that the zero degree direction corresponds to the x-axis, it is seen that for a uniform load, N_x, in the x direction only

$$\varepsilon_x^{\,o} = \frac{\sigma_x^{\,o}}{E_{11}} = A_{11}^{-1}\sigma_x^{\,o}t \tag{4}$$

or therefore

$$E_{11} = \frac{|A|}{t(A_{22}A_{66}-A_{26}A_{26})} \tag{5}$$

Similarly for an applied load of first only N_y, and then only N_{xy}, the elastic moduli E_{22} and G_{12} are

$$E_{22} = \frac{|A|}{t(A_{11}A_{66}-A_{16}A_{16})} \quad , \quad \text{and} \tag{6}$$

$$G_{12} = \frac{|A|}{t(A_{11}A_{22}-A_{12}A_{12})} \quad . \tag{7}$$

Again considering the case of an applied load, N_x, in the x-direction only

$$\varepsilon_x^{\,o} = A_{11}^{-1}\sigma_x^{\,o}t, \quad \text{and}$$

$$\varepsilon_y^{\,o} = A_{12}^{-1}\sigma_x^{\,o}t = -\nu_{12}\varepsilon_x^{\,o},$$

therefore

$$\nu_{12} = -\frac{A_{12}^{-1}}{A_{11}^{-1}} = \frac{A_{12}A_{66}-A_{16}A_{26}}{A_{22}A_{66}-A_{26}A_{26}} \quad . \tag{8}$$

Similarly if $N_y \neq o$, $N_x = N_{xy} = 0$,

$$\varepsilon_y^{\,o} = A_{22}^{-1}\sigma y^{o}t,$$
$$\varepsilon_x^{\,o} = A_{12}^{-1}\sigma_y^{\,o}t = \nu_{21}\varepsilon_y^{\,o},$$

therefore

$$\nu_{21} = -\frac{A_{12}^{-1}}{A_{22}^{-1}} = \frac{A_{12}A_{66}-A_{16}A_{26}}{A_{11}A_{66}-A_{16}A_{16}} \quad . \tag{9}$$

The above equations (5) through (9) are used to compute the average laminate elastic properties E_{11}, E_{21}, G_{12}, ν_{12}, and ν_{21} as given in tables 5 and 6 for all laminates. As mentioned above, the group D hybrid laminates are unsymmetric; however, the degree of non-symmetry is not extreme and is ignored in calculating the elastic constants. The computer program used does, in fact, determine the A_{ij}, B_{ij} and D_{ij} and the ratio of the maximum value of A_{ij} to the maximum value of B_{ij} was found to be $0(10^4)$ for the group D laminates.

III. BUFFER STRIPS PANELS

A. Construction of Panels

The buffer strip panels were fabricated from six layers of style 7500, ten ounce (44 g/cm^2) woven fiber glass cloth in a room temperature cure polyester resin. Style 7500 cloth is woven to have approximately the same properties in the warp (longitudinal direction in the loom) direction as in the fill (transverse direction in the loom) direction as it has 6.5 ends/cm in the warp and 5.5 ends/cm in the filling, with the same fiber used in each direction. The finish on the fabric was Stevens S-910,[4] which gives a good bond with the 33402 Reichhold Tooling polyester resin[5] used.

In constructing the panels, the inner four layers of cloth were placed with the warp direction along the zero degree axis (the axis of load) and the outer layer of cloth on each side of the panel was orientated at $\pm 45°$ from the axis. Each panel was trimed to final dimensions of 30.5 cm by 30.5 cm as shown in Figure 14.

The buffer strips were 2.54 cm wide and 5.08 cm apart and were formed by interrupting the inner four layers of cloth during fabrication and by adding 2.54 cm wide strips of Teflon-coated glass-cloth between layers in

---

[4]Stevens S-910: Registered trademark of J. P. Stevens & Co.

[5]33402 Reichhold Tooling: Registered trademark of Reichhold Chemicals Inc.

the buffer strips. Different degrees of weakening were obtained by using more layers of Teflon-coated glass as indicated in Figure 15 and Table 8.

Five panels as described above were tested with panel E1 being continuous, i.e., no buffer strips, panel E2 had buffer strips formed by interrupting the cloth but did not have the Teflon-coated glass added. Panels E3, E4, and E5 had interrupted buffer strips and in addition had three, five and eight layers of Teflon-coated glass, respectively, added to weaken the inter-laminar bond. Two additional panels, F1 and F2, were fabricated by replacing the interrupted glass cloth at the buffer strips with five ounce (22 g/cm) woven "Kevlar-49" style 281 cloth which has 7 ends/cm in the warp and fill direction. Five ounce Kevlar cloth has approximately the same thickness as the style 7500 glass cloth. Panel F1 had no Teflon-coated glass added and panel F2 had five layers added to each buffer strip in the same manner as panel E4.

All panels had end tabs formed by adding six layers (3 layers on each side) of the 7500 glass to the ends as depicted in Figure (14).

It should be noted that the individual laminae for all of these panels were not fracture tough, i.e., for an initial crack being perpendicular to the load, the load for crack propagation and failure is considerably less than the computed load to failure based on the ultimate stress for an undamaged lamina. This is in direct contrast to the laminates in Part II where all laminae having zero degree

fiber orientation were fracture tough and self-similar crack extension did not occur and the net section stress was approximately σ_{ult}.

B. Test Results

The results of the test on the buffer strip panels are given in Table 8, where it is seen that a significant increase in the ultimate load carrying capacity of the panels, in group F, is obtained as the interface is progressively weakened. Panels F1 and F2 were considerably stronger than panel E1 and approximately the same amount of delamination was observed in F1 as F2 during crack arrest and prior to ultimate failure, indicating that the interlaminar bond for the Kevlar was somewhat weak without the Teflon-coated glass.

Panel E5 supported the largest ultimate load even though it was poorly constructed such that the buffer strips were not straight and the 3.81 cm initial crack was within 0.0492 cm of one buffer strip. Crack initiation began at approximately 35 600N at the near end but arrested upon reaching the buffer strip. Continued increase in the load to 39 140N initiated crack growth at the other end of the notch which also arrested upon reaching the buffer strip. As indicated in Table (8), this panel required a load of 55 600N for ultimate failure. This is about a 25% increase in the load carrying capacity of the panel over panel E1. Panel E2 and E3, even though they did arrest the crack, required little additional load to re-initiate crack extension and had an ultimate failure load less than E1. The

ultimate load for a panel of group E having a width of 30.48 cm - 3.81 cm with no notch was 94 184N. The influence of the notch in panel E5 reduced the ultimate load to 59% of this value and panel E1 carried 46% of the ultimate.

It does then appear that uncoupling the laminae by weakening the interlaminar bond gives a measurable increase in the load carrying capacity of a damaged laminate even for the case of fracture sensitive laminae. Comparing the five panels of group E it is seen that very little change is produced by introducing the buffer strips in E2 or by then weakening the interface between the 0° plies on the buffer strips as shown in Figure 15, (a) and (b). The significant change occurs when the 0° plies in the buffer strips are uncoupled from the $\pm$ 45° plies in panel E4 and E5 and shown in Figure 15, (c) and (d). Replacing the buffer strip material with Kevlar-49 woven cloth as in panels F1 and F2 gave considerable delamination in both cases and the physical appearance of panels F1 and F2 after failure were both similar to panels E4 and E5 in terms of the amount of delamination. The major delamination region in panel F1 was between the resin and the Kevlar at the interface of the buffer strip with the $\pm$45° outer plies. This same region between the $\pm$45° plies and the buffer strip was also the zone of significant delamination in panels E4, E5, and F2.

IV. CONCLUSIONS

These tests demonstrate considerable variation in the mechanical properties of laminates depending on the combination of materials and/or lamina orientation. Classical lamination theory is shown to give a good approximation for the elastic properties for all but the $\pm 45°$ laminates or, therefore, all laminates exhibiting a linear stress/strain relationship.

Observation of the hybrid laminates in Part II of the study and the buffer strip panels of Part III indicate that interlaminar debonding is a significant mechanism associated with fracture toughness and the same delamination process appears to occur when a crack arrests at a buffer strip as takes place in a notched hybrid test coupon. Suitability as a possible candidate for a buffer strip could then initially be determined by fracture test of small notched hybrid coupons.

REFERENCES

1. Verette, R. M. and Labor, J. D., "Structural Criteria for Advanced composite," Northrop Corporation, USAF contract F33615-74-C-5182, Quarterly Reports 1-8, 1974-1976.

2. Poe, C. C., Jr., "Stress-Intensity Factor for a Cracked Sheet with Riveted and Uniformly Spaced Stringers," NASA TR R-358, 1971.

3. Cook, T. S. and Erdogan, F., "Stresses in Bonded Materials with a Crack Perpendicular to the Interface," Int. J. Engr. Science, Vol. 10, (Nov. 1972), pp. 677-697.

4. Erdogan, F. and Biricikoglu, V., "Two Bonded Half-Planes with a Crack Going through the Interface," NASA-TR-72-4, June 1974.

5. Delale, F. and Erdogan, F., "Stress Intensity Factors of Composite Orthotropic Plates Containing Periodic Buffer Strips," NASA CR-145355, 1978.

6. Goree, J. G. and Venezia, W. A., "Bonded Elastic Half-Planes with an Interface Crack and a Perpendicular Intersecting Crack that Extends into the Adjacent Material - Part I," Int. J. Engr. Science, Vol. 1, (Jan. 1977), pp. 1-17.

7. Goree, J. G. and Venezia, W. A., " Bonded Elastic Half-Planes with an Interface Crack and a Perpendicular Intersecting Crack that Extends into the Adjacent Material - Part II," Int. J. Engr. Science, Vol. 1, (Jan. 1977), pp. 19-27.

8. Jones, R. M., "Mechanics of Composite Materials," Scripta Book Co., Washington, DC, 1975.

9. Pagano, N. J. and Pipes, R. B., "Some Observations on the Interlaminar Strength of Composite Laminates," Int. J. Mech. Sci., Vol. 15 (1973), pp. 679.

10. Pagano, N. J., "On the Calculation of Interlaminar Normal Stress in Composite Laminates," J. Comp. Mat., Vol. 8, (1974), pp. 65.

11. Hedgepeth, J. M., "Stress Concentrations in Filamentary Structures," NASA TN D-882, May 1971.

12. Hedgepeth, J. M. and Van Dyke, P., "Local Stress Concentrations in Imperfect Filamentary Composite Materials," J. Comp. Mat., Vol. 1, (1967), pp. 294-309.

13. Eringen, A. C. and Kim. B. S., "Stress Concentrations in Filamentary Composites with Broken Fibers," Princeton University Tech. Report No. 36, (Sept. 1973), ONR Contract N-00014-67-A-0151-0004.

14. Newman, J. C., Jr., "An Improved Method of Collocation for the Stress Analysis of Cracked Plates with Various Shaped Boundaries," NASA TN D-6376, (August 1971).

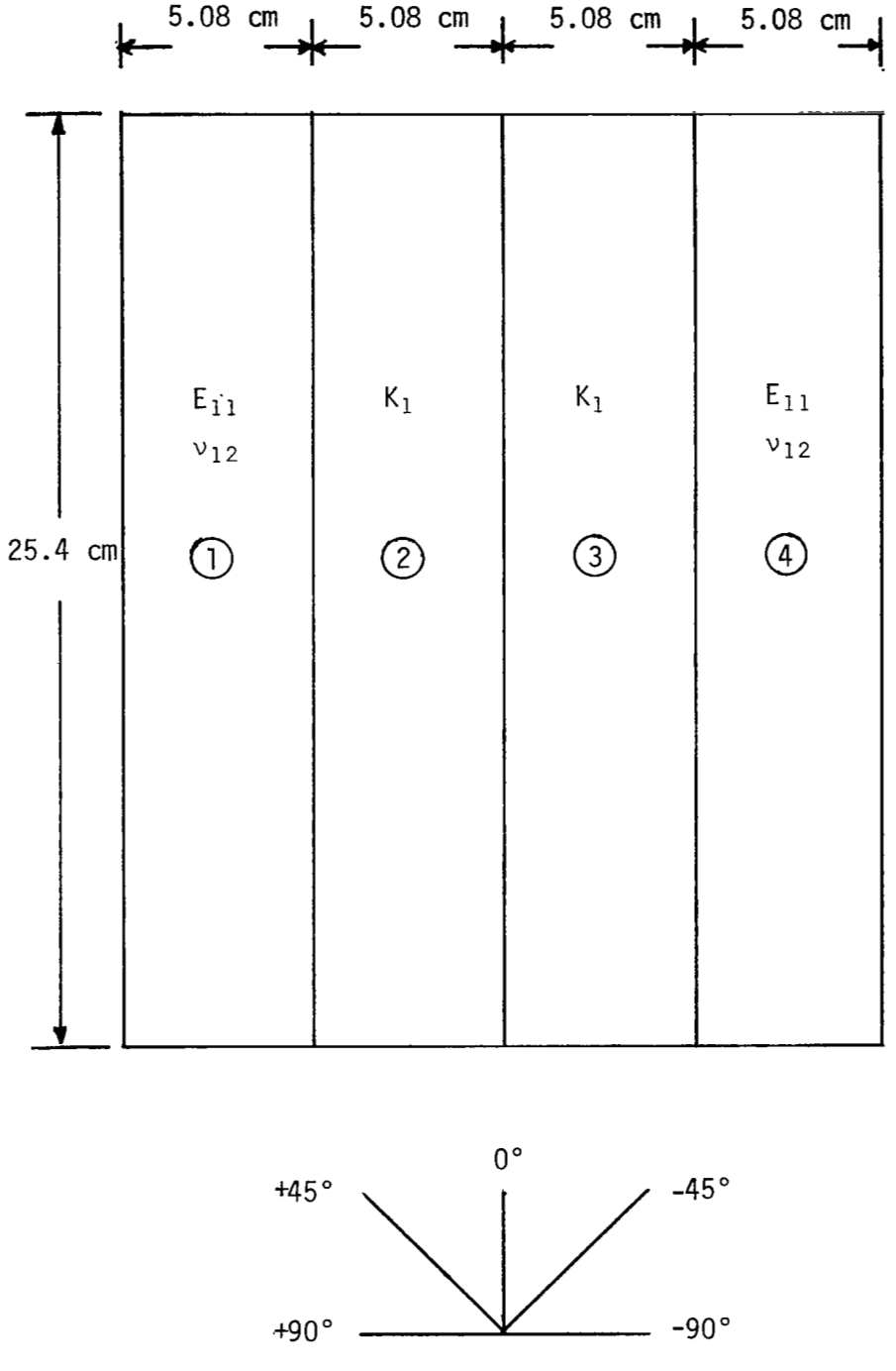

Figure 1. Coupon Designation for Panels in Groups A and B

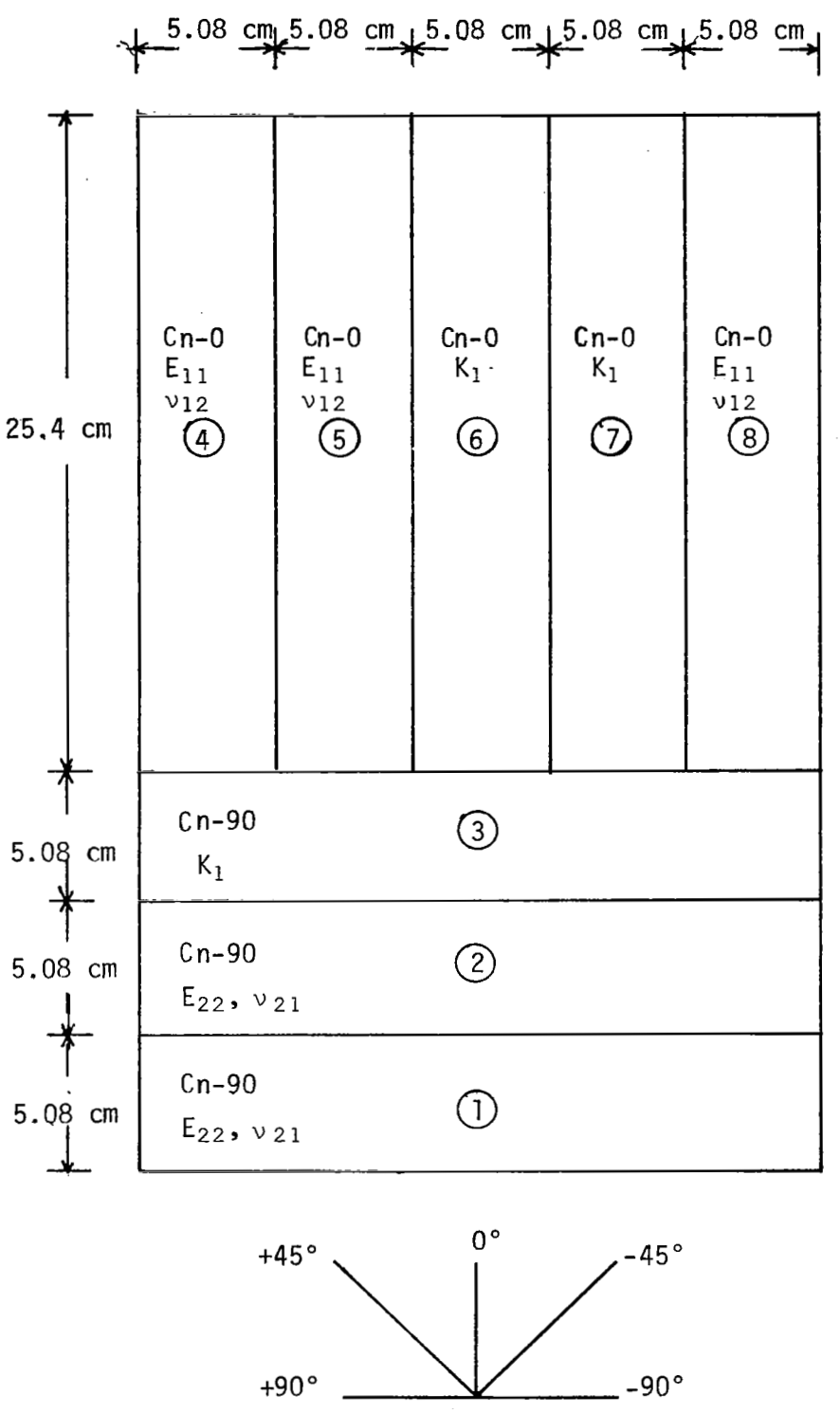

Figure 2. Coupon Designation for Panels in Groups C and D

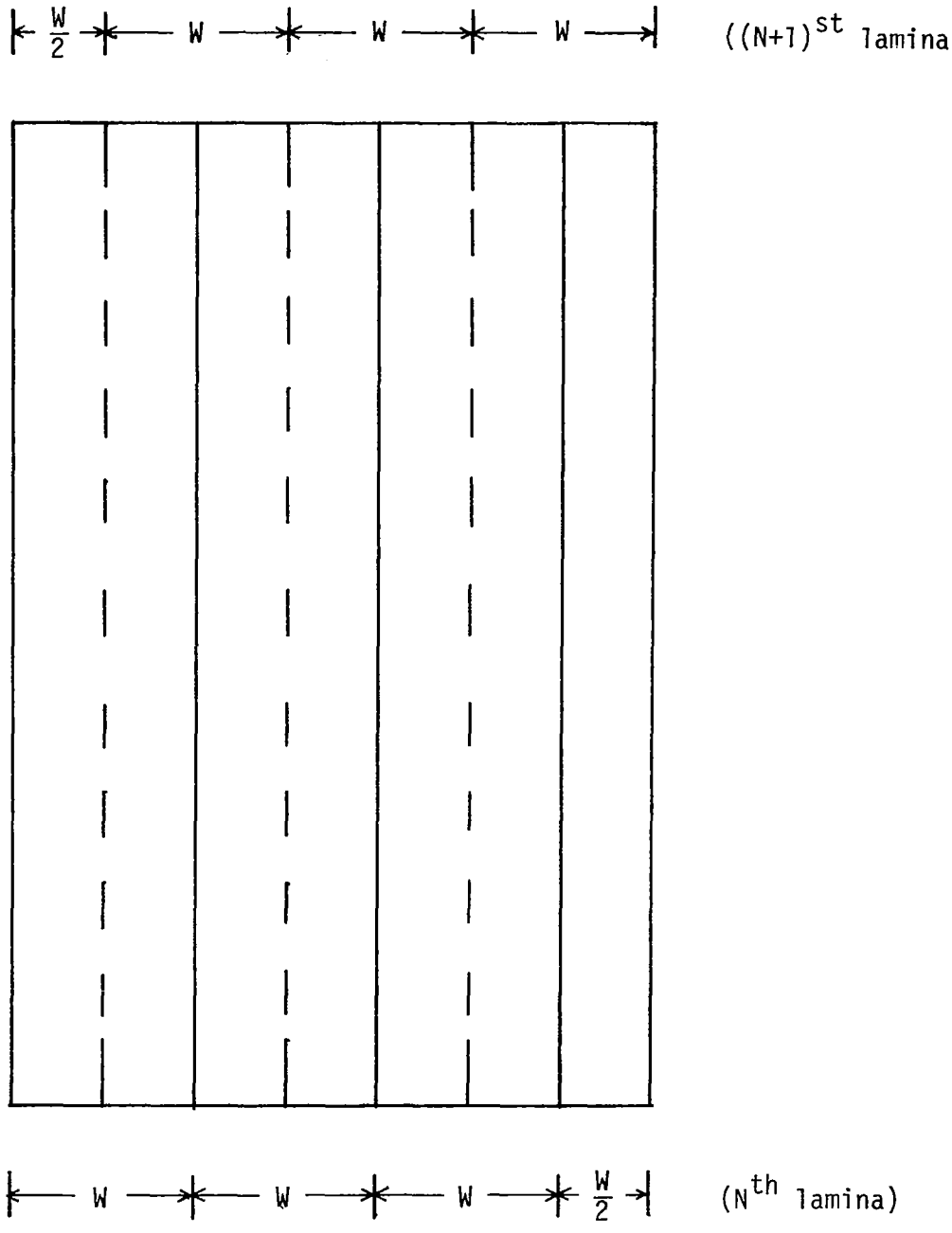

Figure 3. Top View of the Alternating Laminae in the Unidirectional Panels of Group A
w = tape width = 7.62 cm
N = 1, 3, 5, 7

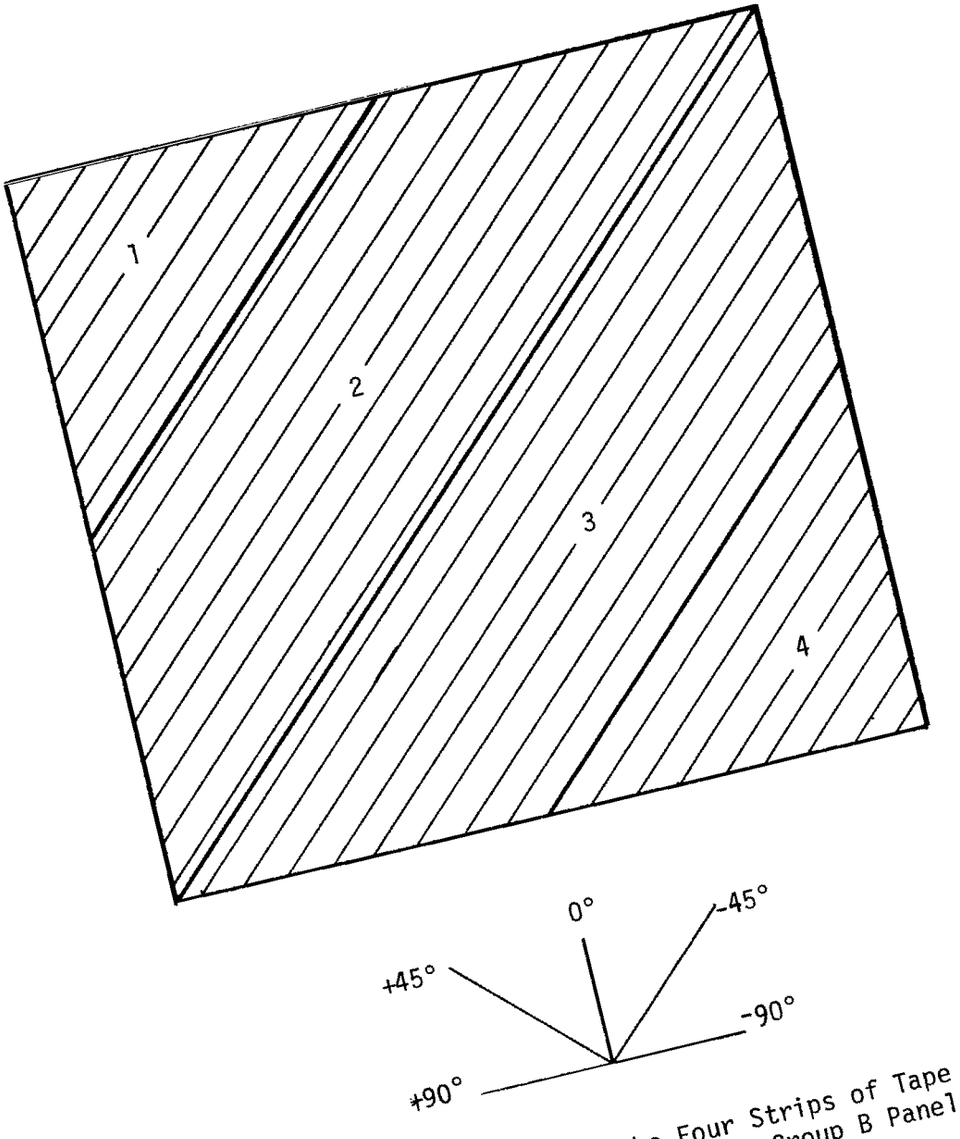

Figure 4. Top View of the Four Strips of Tape in a 45° Lamina in the Group B Panels

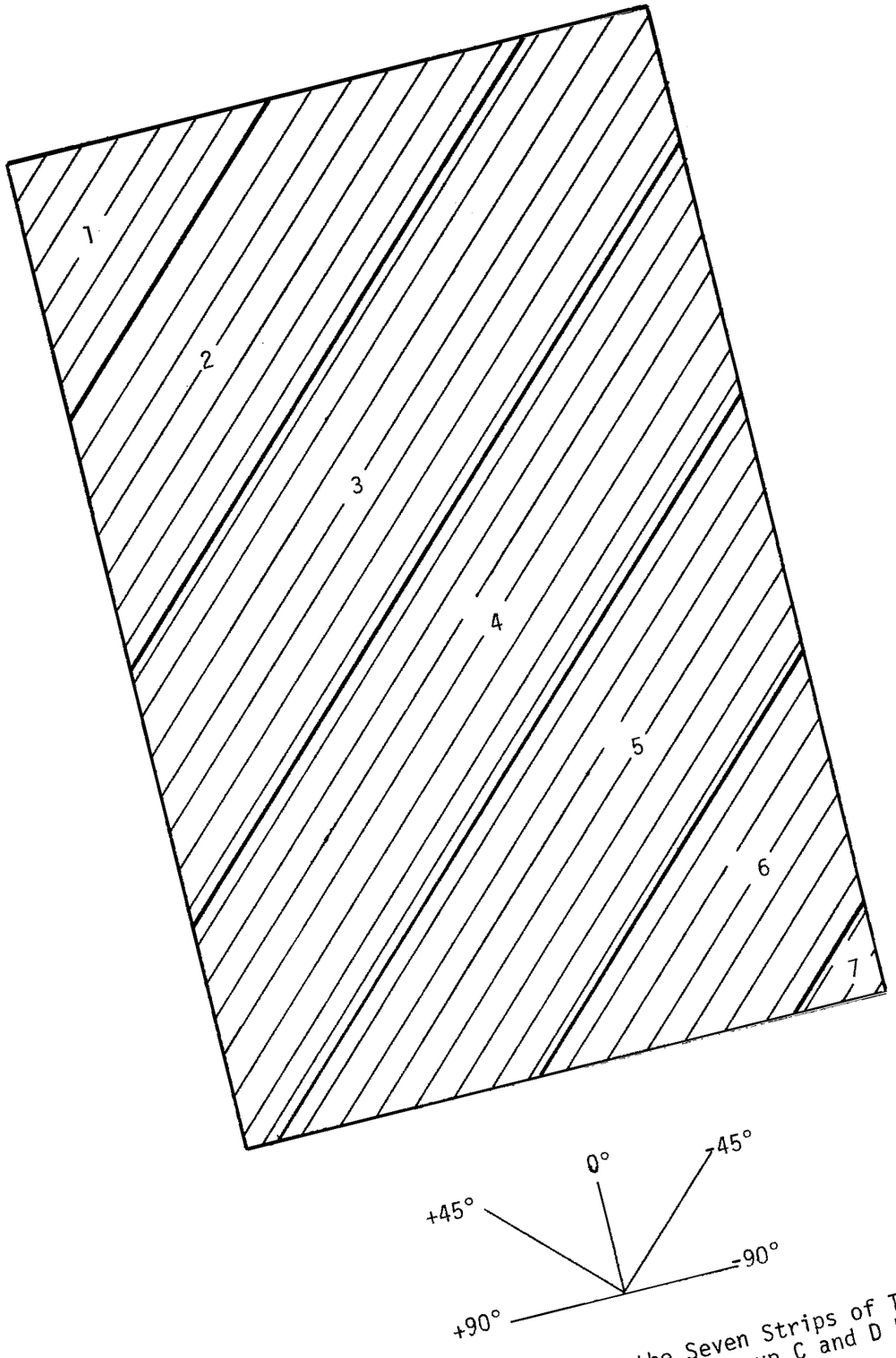

Figure 5. Top View of the Seven Strips of Tape in a 45° Ply in the Group C and D Panels

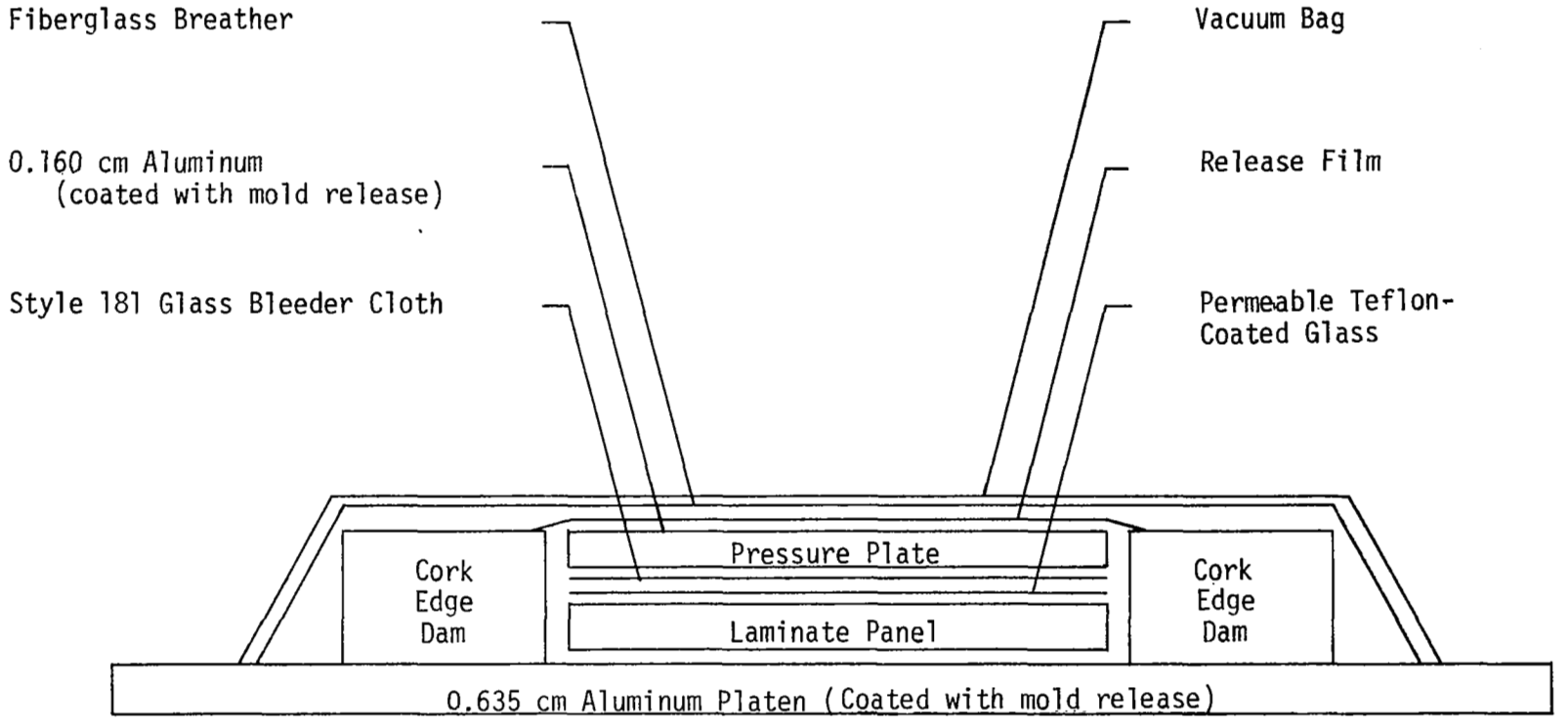

Figure 6. Curing Method for Hybrid/Graphite/Epoxy Laminates

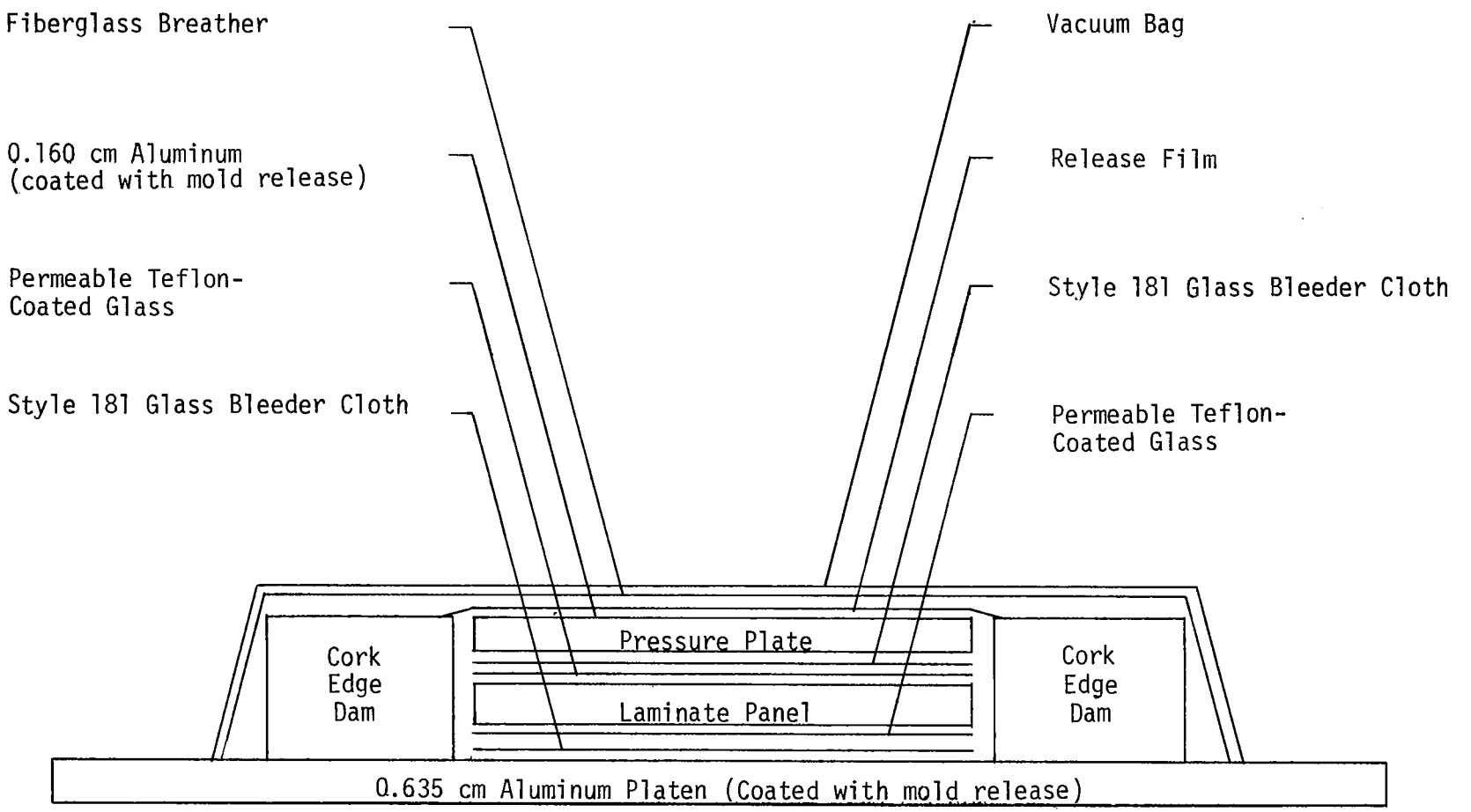

Figure 7. Modified Curing Method for Hybrid/Graphite/Epoxy Laminates

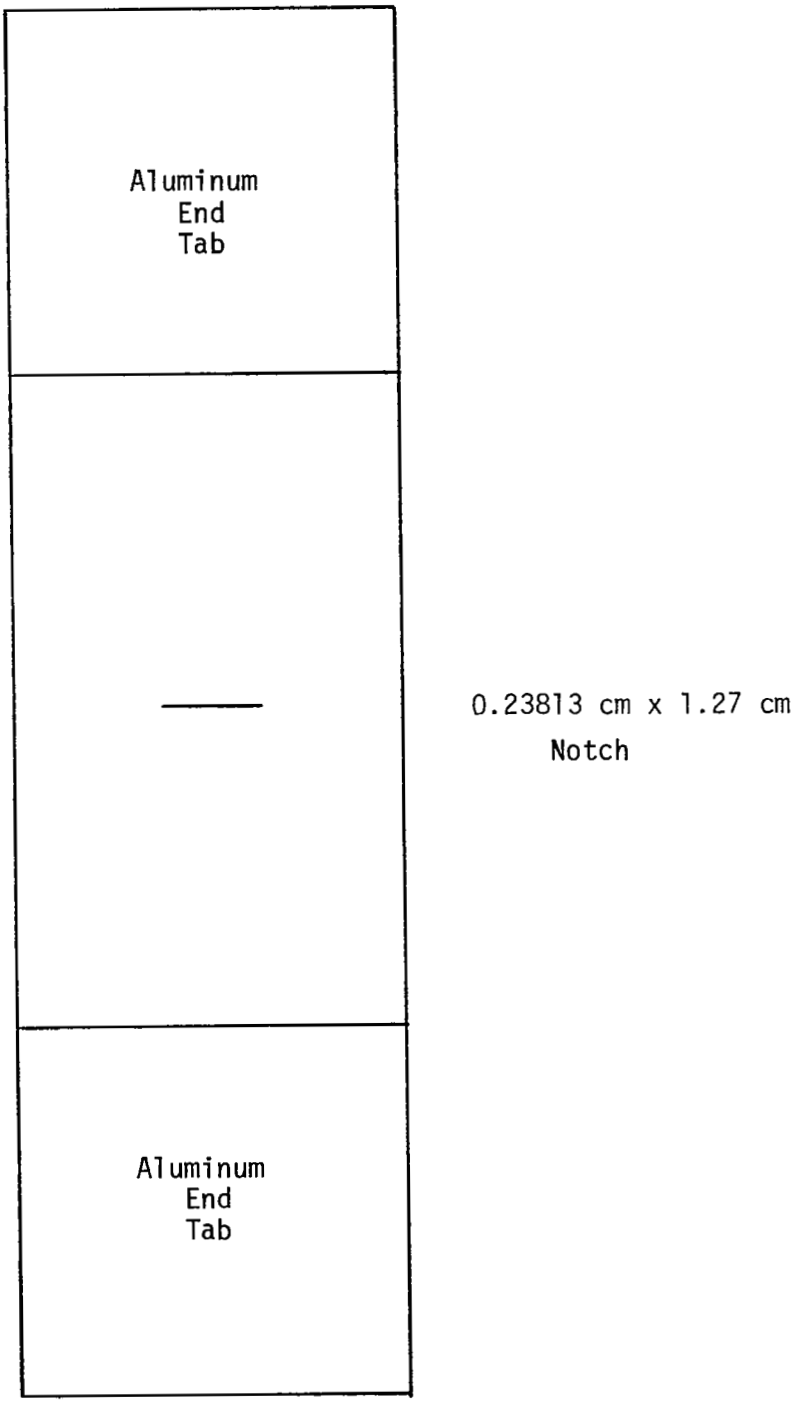

Figure 8. Test Specimen with Through-the-Laminate Center Notch for Determining Stress Intensity Factor, K_1

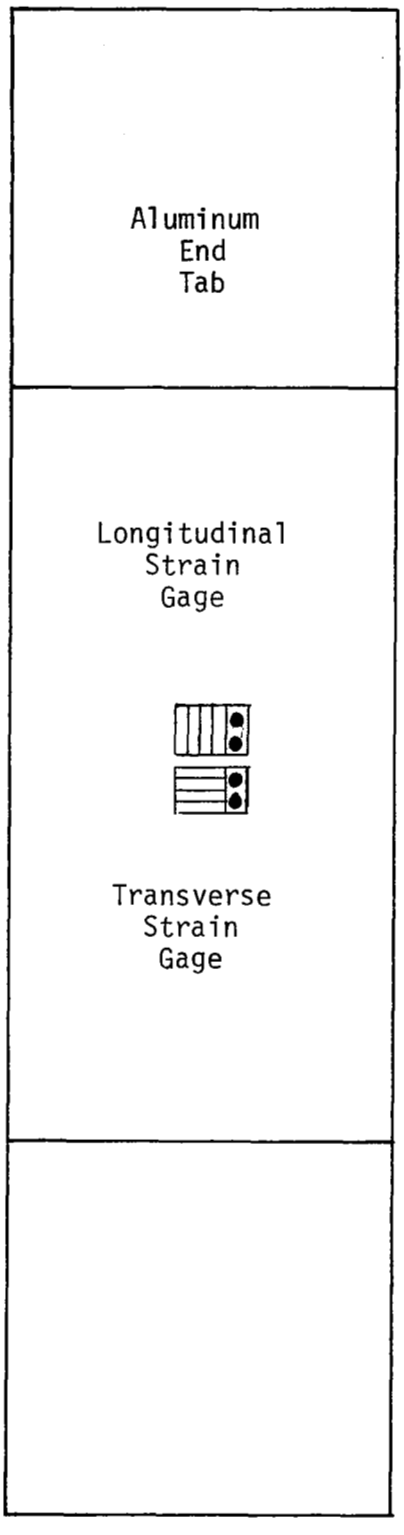

Figure 9. Test Specimen for Obtaining Stress/Strain Relationships

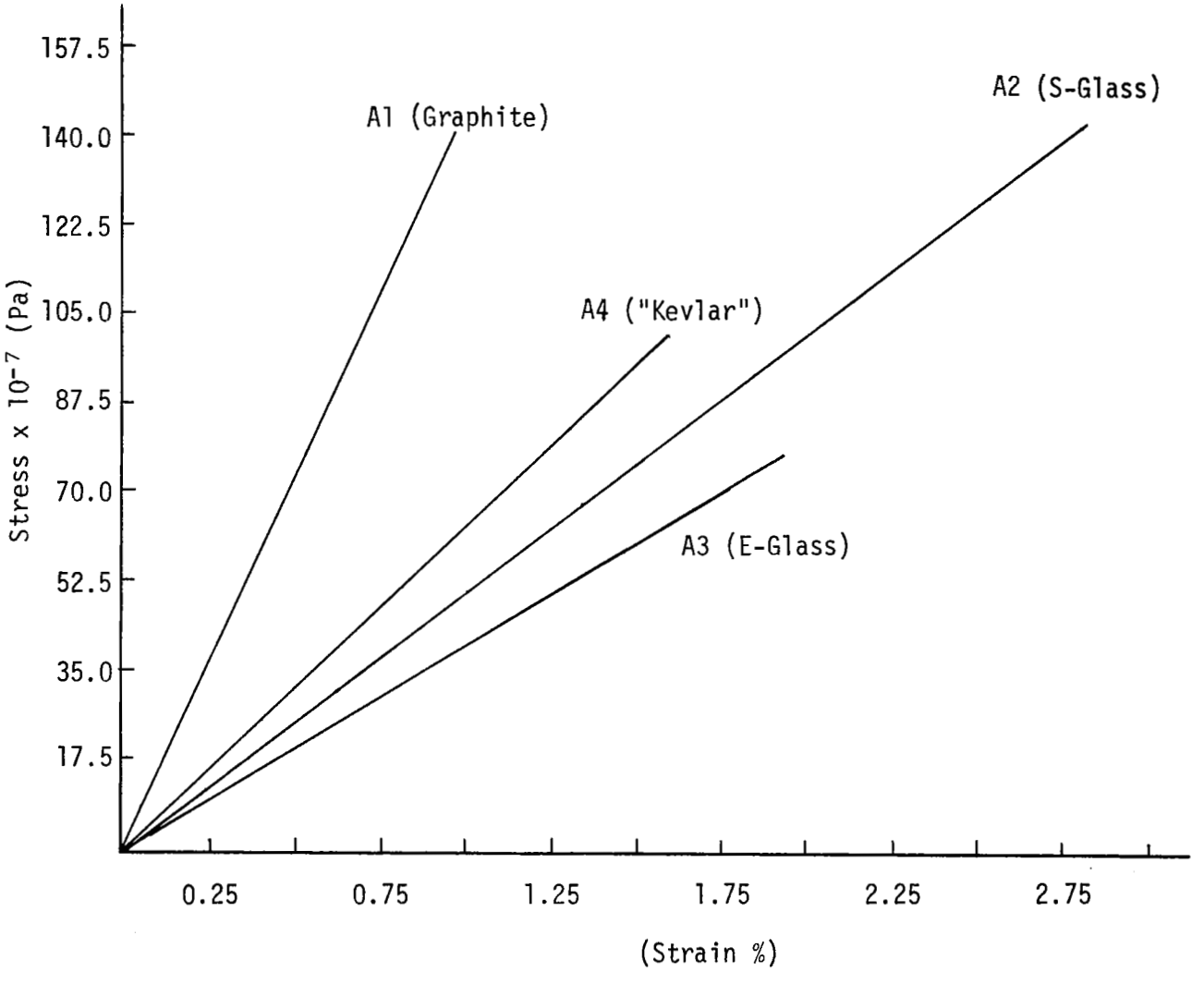

Figure 10. Tensile Stress/Strain Curves (E_{11}) for the Unidirectional Laminates of Group A

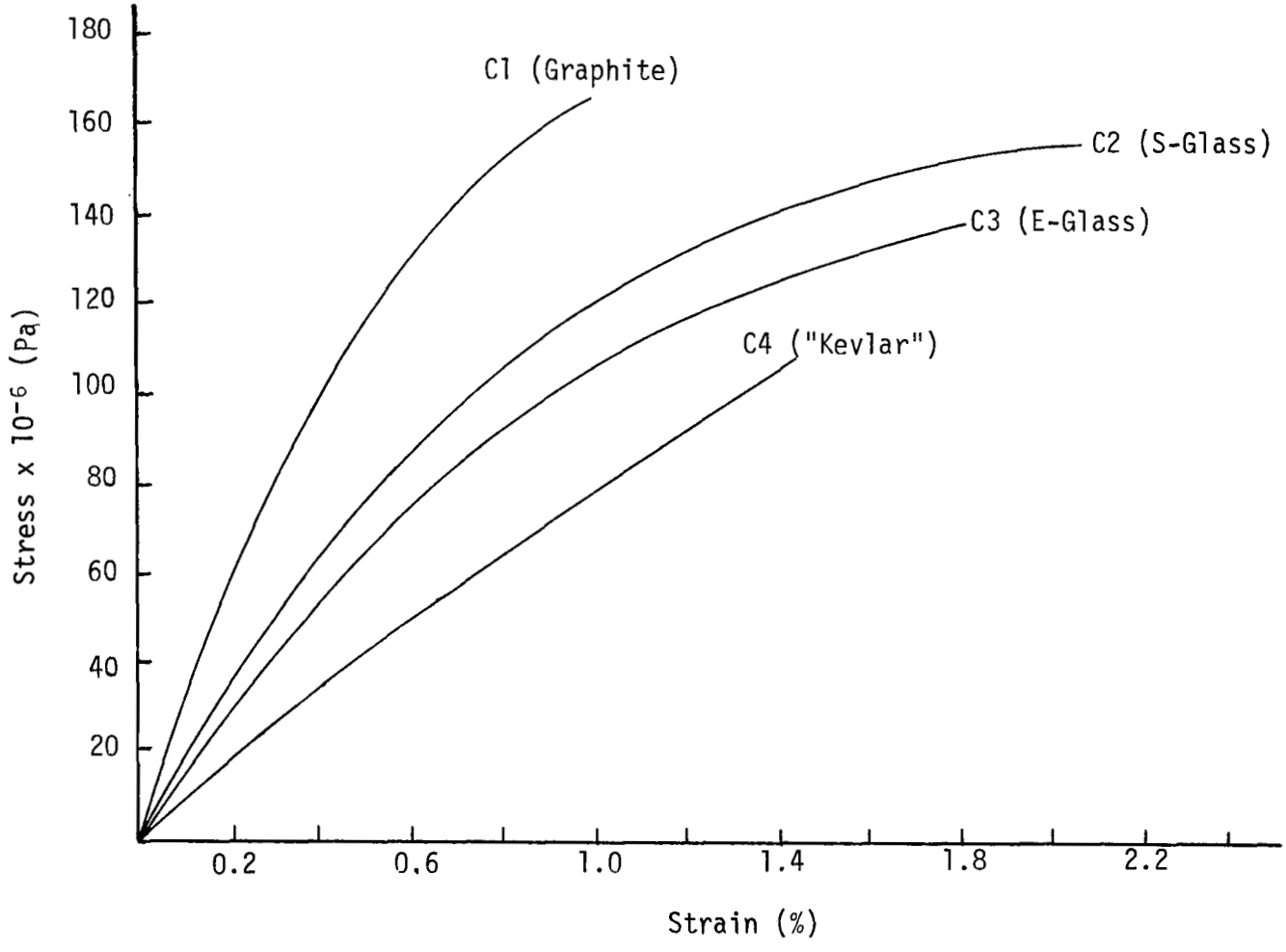

Figure 11. Tensile Stress/Strain Curves (E_{11}) for the $\pm$ 45 Degree Laminates of Group B

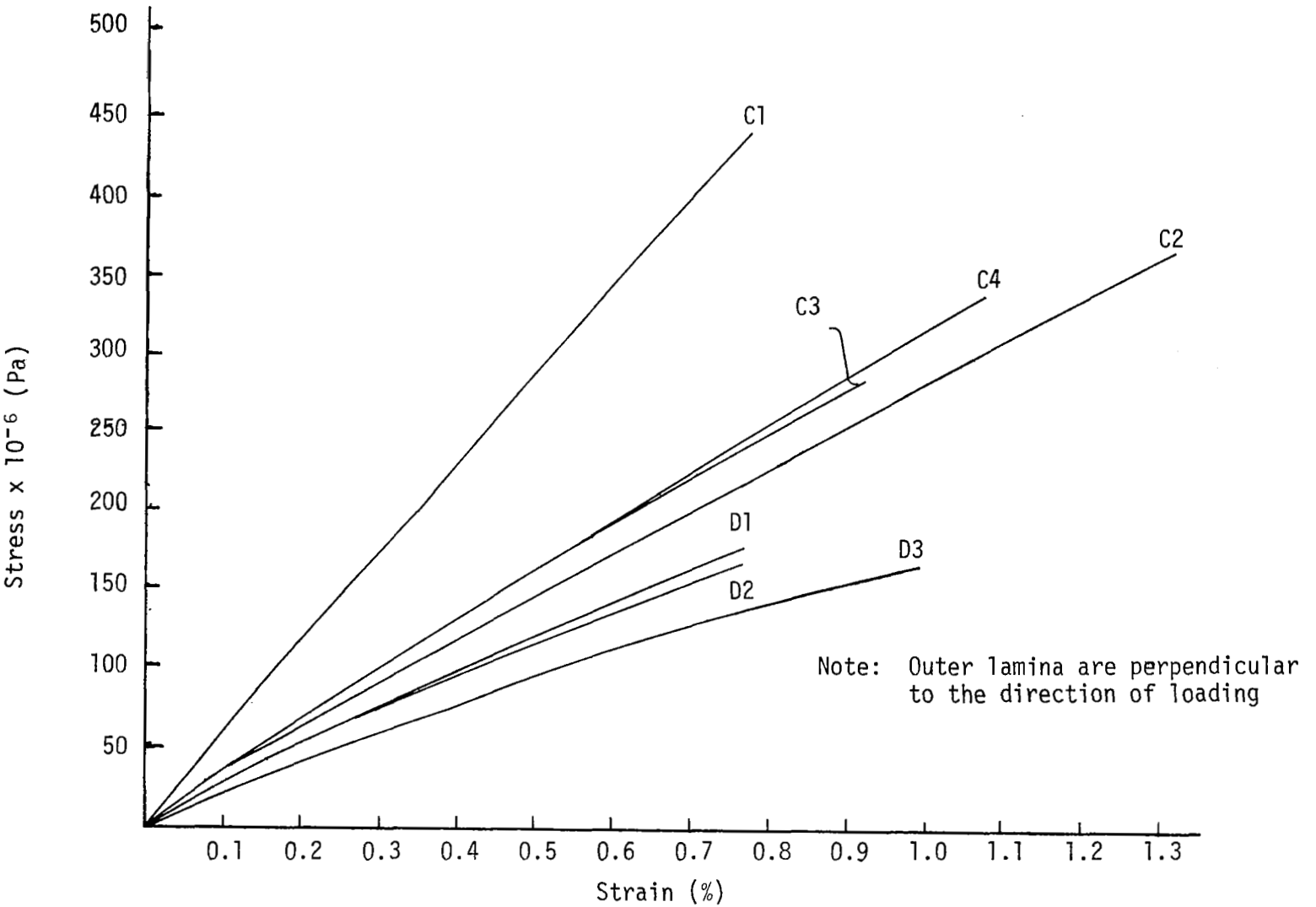

Figure 12. Tensile Stress/Strain Curves (E_{11}) of Eight Ply Multidirectional Laminates of Groups C and D

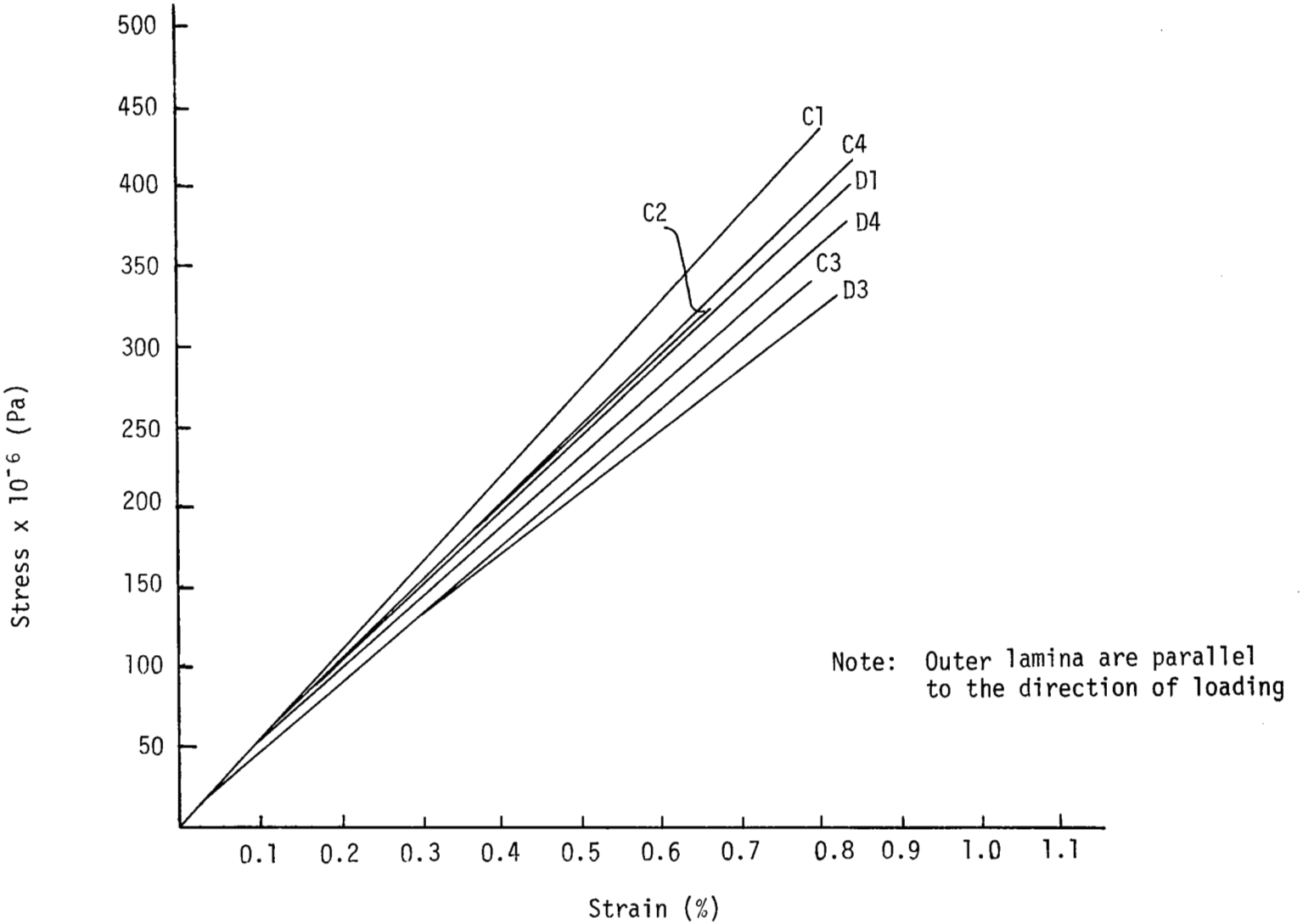

Figure 13. Tensile Stress/Strain Curves (E_{22}) of Eight Ply Multidirectional Laminates of Groups C and D

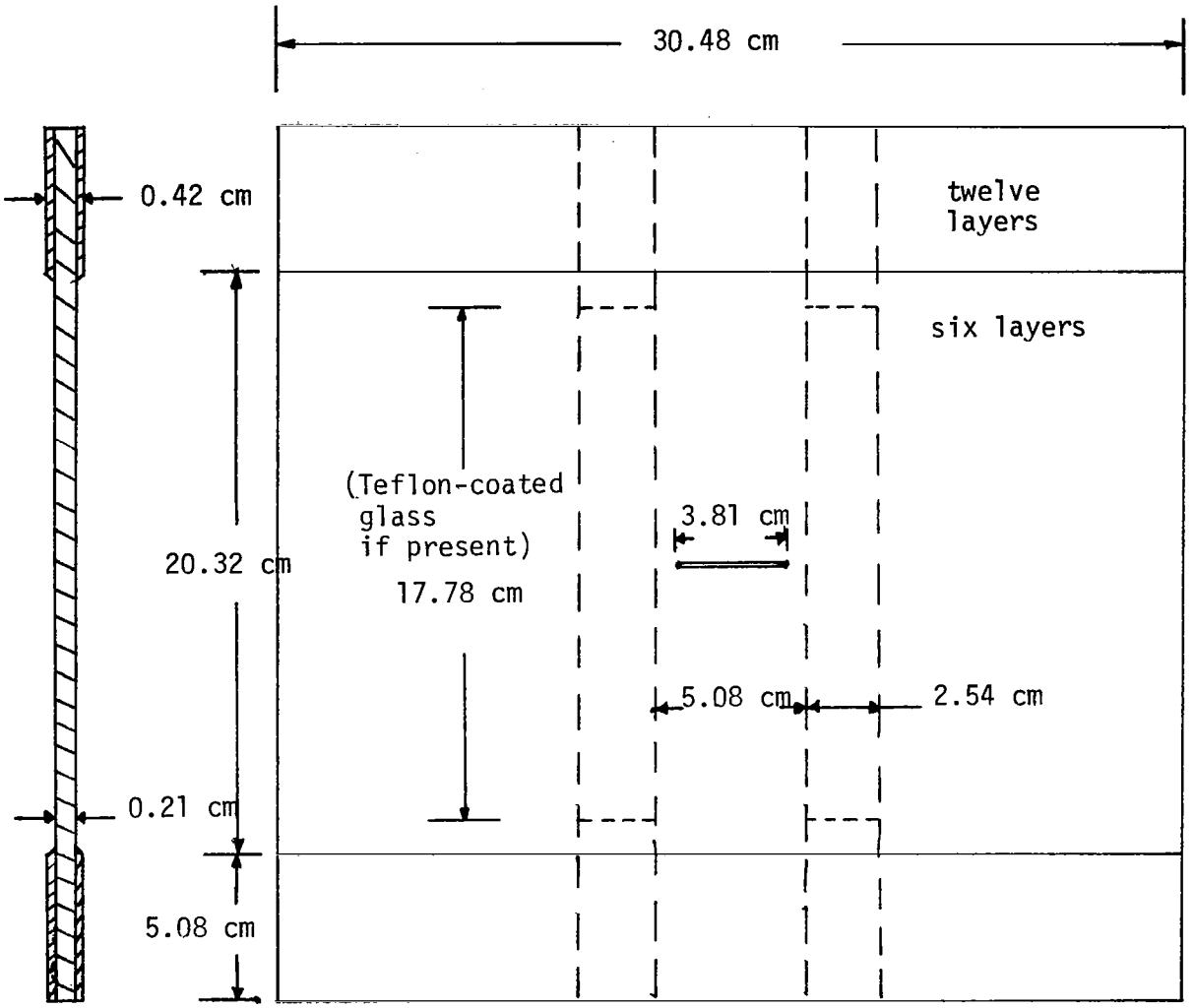

Figure 14. Buffer Strip Panels

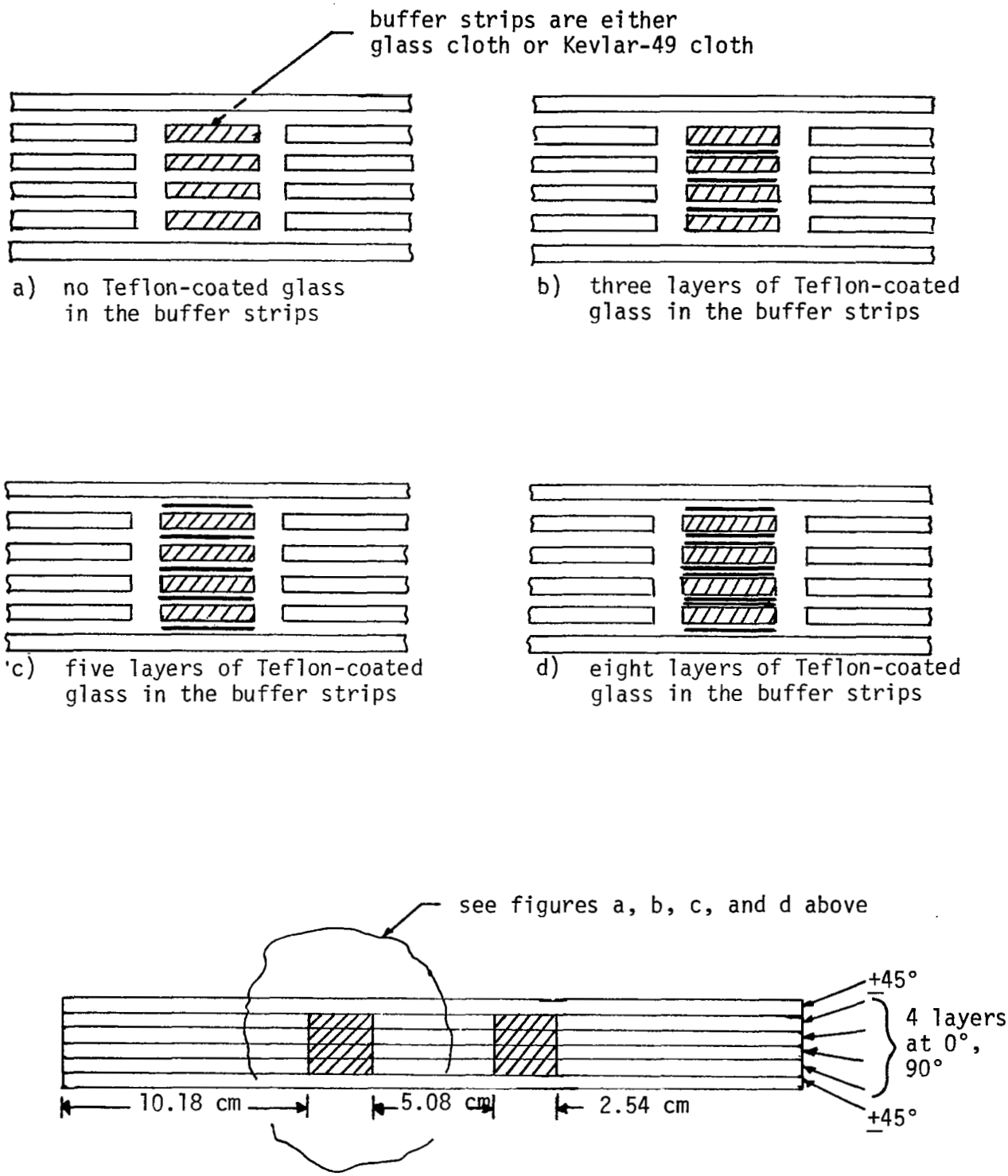

Figure 15. Placement of the Teflon-Coated Glass in the Buffer Strips

Table 1. Construction of the Laminate Panels

Laminate Panel		
A1	5.08 cm x 20.32 cm x 0.110 cm	All Graphite $[0°]_8$
A2	5.08 cm x 20.32 cm x 0.115 cm	All S-glass $[0°]_8$
A3	5.08 cm x 20.32 cm x 0.195 cm	All E-glass $[0°]_8$
A4	5.08 cm x 20.32 cm x 0.120 cm	All "Kevlar" $[0°]_8$
B1	5.08 cm x 20.32 cm x 0.114 cm	All Graphite $[(\pm 45°)_2]_S$
B2	5.08 cm x 20.32 cm x 0.117 cm	All S-glass $[(\pm 45°)_2]_S$
B3	5.08 cm x 20.32 cm x 0.202 cm	All E-glass $[(\pm 45°)_2]_S$
B4	5.08 cm x 20.32 cm x 0.126 cm	All "Kevlar" $[(\pm 45°)_2]_S$
C1	5.08 cm x 25.4 cm x 0.109 cm	All Graphite $[90°, \pm 45°, 0°]_S$
C2	5.08 cm x 25.4 cm x 0.114 cm	0° Plies replaced by 0° S-glass
C3	5.08 cm x 25.4 cm x 0.141 cm	0° " " " 0° E-glass
C4	5.08 cm x 25.4 cm x 0.114 cm	0° " " " 0° "Kevlar"
D1	5.08 cm x 25.4 cm x 0.119 cm	0° $\pm 45°$ Graphite
D2	5.08 cm x 25.4 cm x 0.118 cm	0° " " " $\pm 45°$ S-glass
D3	5.08 cm x 25.4 cm x 0.145 cm	0° " " " $\pm 45°$ E-glass
D4	5.08 cm x 25.4 cm x 0.117 cm	0° " " " $\pm 45°$ "Kevlar"

Table 2. Per Cent Fiber by Weight of the Uncured Preimpregnated Tape Used in Construction of the Laminate Panels

Tape	Experimental Results (%)	NARMCO Report (%)
E-Glass	59.75	56
"Kevlar" 49	57.96	55
1014 S-Glass	64.78	65
T-300 Graphite	62.28	62

Table 3. Autoclave Cycle Recommended by Narmco Materials Inc. for Curing Graphite Parts

Step	Procedure
1. Initial Pressure	22 inches Hg. Vacuum (74.29 kPa)
2. Initial Heat Rise	Room temperature to 135 ± 3°C at 2-3°C/min
3. Dwell	60 minutes beginning at 129°C
4. Pressurize	Apply 586 to 689 kPa Vent vacuum at 138 kPa
5. Final Heat Rise	118 ± 3°C to 179 ± 3°C at 2-3°C/min
6. Cure	120 ± 5 minutes at 179 ± 6°C
7. Cooling	Cool to 60°C or below under pressure

Table 4. Autoclave Cycle Used With the Modified Curing Method for Graphite Parts

1.	Initial Pressure	29 inches Hg. Vacuum (98 kPa)
2.	Initial Heat Rise	Room temperature to 121 ± 3°C
3.	Pressurize	Begin pressurizing at 121°C Apply 414 kPa prior to obtaining 132°C
4.	Final Heat Rise	0.6°C/min to 179 ± 3°C
5.	Cure	120 minutes at 179 ± 3°C, 414 kPa and 29 inches Hg (98 kPa)
6.	Cooling	Cool to 140°F (60°C) under pressure

Table 5. Moduli of Elasticity and Poisson's Ratios for the Single Material Laminates (A and B)

Unidirectional Laminates ($[0°]_8$, same material, 5.08 cm wide)

Laminate	Thickness	E_{11} x 10^{-9} Pa	E_{22} x 10^{-9} Pa	ν_{12}	ν_{21}	G_{12} x 10^{-9} Pa
A1(Graphite)	0.110 cm	[1]142.52	[2]11.72	[1]0.32	[3]0.026	[2]4.48
A2(S-Glass)	0.115 cm	[1] 51.02	[2]11.03	[1]0.29	[3]0.063	[2]4.48
A3(E-Glass)	0.195 cm	[1] 43.44	[2]10.34	[1]0.30	[3]0.071	[2]2.41
A4(Kevlar-49)	0.120 cm	[1] 62.54	[2] 5.52	[1]0.39	[3]0.034	[2]2.07

Forty-Five Degree Laminates ($[\pm45°]_4$, same material, 5.08 cm wide)

Laminate	Thickness	E_{11} x 10^{-9} Pa	$E_{22} = E_{11}$	ν_{12}	$\nu_{21} = \nu_{21}$	G_{12} x 10^{-9} Pa
B1(Graphite)	0.114 cm	[1]27.24 [4]16.13		[1]0.88 [4]0.80		[4]37.03
B2(S-Glass)	0.117 cm	[1]19.72 [4]14.27		[1]0.57 [4]0.59		[4]14.13
B3(E-Glass)	0.202 cm	[1]13.79 [4] 8.34		[1]0.53 [4]0.73		[4]12.14
B4(Kevlar-49)	0.126 cm	[1] 7.86 [4] 7.45		[1]0.90 [4]0.80		[4]16.13

[1] Experimental value

[2] Average values given by the vendor

[3] $\nu_{21} = \nu_{12}E_{22}/E_{11}$

[4] Computed using CLT [8]

Table 6. Moduli of Elasticity and Poisson's Ratios for the Hybrid Laminates (C and D)

Hybrid Laminates ([90°,±45°,-,-,±45°,90°], 5.08 cm wide)

Laminate	Thickness	$E_{11} \times 10^{-9}$ Pa	$E_{22} \times 10^{-9}$ Pa	ν_{12}	ν_{21}	$G_{12} \times 10^{-9}$ Pa
C1 (Graphite) 0°,0°	0.109 cm	[1] 50.26	[1] 55.50	[1] 0.32	[1] 0.31	[2] 20.75
		[2] 55.02	[2] 55.02	[2] 0.32	[2] 0.32	
C2 (S-Glass) 0°,0°	0.114 cm	[1] 30.00	[1] 53.02	[1] 0.30	[1] 0.47	[2] 20.75
		[2] 31.79	[2] 51.09	[2] 0.32	[2] 0.52	
C3 (E-Glass) 0°,0°	0.141 cm	[1] 32.54	[1] 45.99	[1] 0.41	[1] 0.43	[2] 17.24
		[2] 32.41	[2] 45.09	[2] 0.32	[2] 0.45	
C4 (Kevlar-49) 0°,0°	0.114 cm	[1] 32.54	[1] 53.02	[1] 0.31	[1] 0.41	[2] 20.13
		[2] 34.96	[2] 50.68	[2] 0.33	[2] 0.47	
D1 (Graphite) ±45°	0.119 cm	[1] 26.75	[1] 50.82	[1] 0.38	[1] 0.60	[2] 28.89
		[2] 25.58	[2] 48.40	[2] 0.40	[2] 0.76	
D2 (S-Glass) ±45°	0.118 cm	[1] 26.75	[1] ——	[1] 0.33	[1] ——	[2] 23.17
		[2] 23.31	[2] 47.99	[2] 0.35	[2] 0.72	
D3 (E-Glass) ±45°	0.145 cm	[1] 18.62	[1] 43.09	[1] 0.32	[1] 0.64	[2] 20.89
		[2] 20.20	[2] 40.06	[2] 0.37	[2] 0.74	
D4 (Kevlar-49) ±45°	0.117 cm	[1] ——	[1] 45.99	[1] ——	[1] 0.69	[2] 23.65
		[2] 22.27	[2] 46.20	[2] 0.36	[2] 0.75	

[1] Experimentally determined value

[2] Computed from C.L.T. [8]

Table 7. Notch Sensitivity Factors, Unnotched Ultimate Stress, Notched Ultimate Average Stress, and Net Section Average Stress of the Coupons.[1]

Coupon	K_I (KPa$\sqrt{m}$)	[1]σ_u (KPa)	[2]σ_{nu} (KPa)	[3]σ_n (KPa)
A1	—	1 404 356	—	—
A2	—	1 443 330	—	—
A3	76 498	748 452	524 771	715 322
A4	157 565	1 026 038	726 230	1 027 320
B1	13 178	163 756	90 408	120 531
B2	20 386	199 831	139 853	186 599
B3	15 053	136 321	103 259	137 824
B4	12 097	104 597	82 981	110 906
C1-0	31 477	445 038	215 931	287 666
C2-0	35 520	371 641	243 890	325 189
C3-0	31 575	279 379	216 606	288 956
C4-0	35 493	339 448	243 483	324 755
D5-0	23 750	180 035	162 922	217 299
D6-0	24 849	176 098	170 409	227 245
D7-0	20 288	163 177	139 251	185 607
D8-0	—	—	—	—
C1-90	31 539	442 149	216 365	288 439
C2-90	26 175	326 637	179 560	239 408
C3-90	26 536	336 986	182 042	242 683
C4-90	26 536	419 837	184 772	246 655
D5-90	26 731	401 854	183 379	244 504
D6-90	—	—	—	—
D7-90	20 939	322 215	143 644	191 529
D8-90	27 204	382 527	186 620	248 496

[1] σ_u = Ultimate stress of the un-notched coupons = Pult/wt

[2] σ_{nu} = Ultimate average stress of the center notched coupons = Pult/wt

[3] σ_n = Net section average stress of the center notched coupons = Pult/(w-2a)t

Table 8. Buffer Strip Panels

panel[1]	buffer strip material	Teflon-coated Glass	initial crack length	crack initiation load	Ultimate load
E1[2]	Style 7500 woven cloth 10 oz.	No	3.81 cm	43 590N	43 590N
E2	Style 7500 woven cloth 10 oz.	No	3.81 cm	39 934N	41 811N
E3	Style 7500 woven cloth 10 oz.	3 layers	3.81 cm	37 808N	42 258N
E4	Style 7500 wovencloth 10 oz.	5 layers	3.81 cm	40 032N	51 152N
E5	Style 7500 woven cloth 10 oz.	8 layers	3.81 cm	35 584N	55 600N
F1	Kevlar-49 woven cloth 5 oz.	No	3.81 cm	42 701N	54 710N
F2	Kevlar-49 woven cloth 5 oz.	5 layers	3.81 cm	41 589N	51 152N

[1] outside layers for all panels was ± 45° style 7500, 10 oz. glass

[2] panel E1 was constructed of continuous cloth, i.e., not cut at the buffer strips

1. Report No.	2. Government Accession No.	3. Recipient's Catalog No.
NASA CR-3000		

4. Title and Subtitle	5. Report Date
Preliminary Investigation of Crack Arrest in Composite Laminates Containing Buffer Strips	May 1978
	6. Performing Organization Code

7. Author(s)	8. Performing Organization Report No.
James G. Goree	
	10. Work Unit No.

9. Performing Organization Name and Address	11. Contract or Grant No.
Clemson University Clemson, S.C. 29631	NSG-1297
	13. Type of Report and Period Covered
12. Sponsoring Agency Name and Address	Contractor Report
National Aeronautics and Space Administration Washington, D.C. 20546	14. Sponsoring Agency Code 743-01-03-02

15. Supplementary Notes

Langley Technical Monitor: Clarence C. Poe, Jr.

Topical Report.

16. Abstract

The mechanical properties of some hybrid buffer strip laminates and the crack arrest potential of laminates containing buffer strips were determined.

The hybrid laminates consisted of graphite with either S-glass, E-glass, or Kevlar. Unnotched tensile coupons and center-cracked fracture coupons were tested. Elastic properties, complete stress/strain curves, and critical stress intensity values are given. The measured elastic properties compare well with those calculated by classical lamination theory for laminates with linear stress/strain behavior. The glass hybrids had more delamination and higher fracture toughness than the all-graphite or the Kevlar hybrid.

The buffer strip laminates for the crack arrest study were fabricated using six layers of woven fiberglass cloth and polyester resin. Each laminate contained two buffer strips formed by interrupting the cloth and weakening the inner laminar bond with teflon coated glass fabric. Woven Kevlar cloth was also used in some laminates in place of the fiberglass buffer strips. Results indicate that a weak interface bond does enhance crack arrest.

17. Key Words (Suggested by Author(s))	18. Distribution Statement
Composite materials buffer strips fracture crack arrest tests	Unclassified - Unlimited Subject Category 39

19. Security Classif. (of this report)	20. Security Classif. (of this page)	21. No. of Pages	22. Price*
Unclassified	Unclassified	58	$5.25

*For sale by the National Technical Information Service, Springfield, Virginia 22161

NASA-Langley, 1978